Characteristic Impedance of a Wide Slotline on Low-Permittivity Substrates

R. JANASWAMY, STUDENT MEMBER, IEEE, AND
D. H. SCHAUBERT, SENIOR MEMBER, IEEE

Abstract —Computed results on the characteristic impedance of wide slots etched on an electrically thin substrate of low dielectric constant ϵ_r are presented. These results combined with those in [1] provide design data for these slotlines. Curves are presented for $\epsilon_r = 2.22$, 3.0, 3.8, and 9.8. Comparison is shown for the characteristic impedance between the present calculations and those available in the literature for high-ϵ_r substrates. Empirical formulas, based on least-square curve fitting, are presented for the normalized slot wavelength λ'/λ_0 and the characteristic impedance Z_0 over the range $0.0015 \leq W/\lambda_0 \leq 1.0$, $0.006 \leq d/\lambda_0 \leq 0.06$, $2.22 \leq \epsilon_r \leq 9.8$.

I. Introduction

Impedance properties of a slotline (shown in Fig. 1) have been thoroughly treated in the literature by a number of authors [2], [3]. All the previous work has been confined to slots on high-ϵ_r substrates ($\epsilon_r \geq 9.6$), which are typically used for circuit applications. No data have been reported for slots on low-ϵ_r substrates, where slotlines have interesting applications as antennas [4]–[6]. Knowledge of the characteristic impedance of slotlines on these low-ϵ_r substrates is highly desirable in designing a proper feed and accompanying circuits for these antennas.

In this paper, computed data are presented for the characteristic impedance Z_0 for slots on low-ϵ_r substrates. The problem is formulated in the spectral domain, and the eigenvalue equation for the eigenpair (λ', e^s), where λ' is the slot wavelength and e^s the slot field, is solved by using the spectral Galerkin's method [7]. The slot characteristic impedance Z_0 is calculated in the spectral domain from the slot field.

II. Formulation of the Problem and Numerical Results

The characteristic impedance Z_0 of the slotline shown in Fig. 1 is defined as [2]

$$Z_0 = \frac{|V_0|^2}{P_f} \tag{1}$$

where V_0 is the voltage across the slot in the plane of the slot and is given in terms of the transverse electric field component E_x as

$$V_0 = \int_{-W/2}^{W/2} E_x \, dx = \tilde{E}_x(\alpha)|_{\alpha=0} = \tilde{E}_x(0) \tag{2}$$

where the tilde denotes quantities Fourier transformed with respect to the x-axis, and α is the transform variable. P_f is the real part of the complex power flow (actually real in this case for a propagating mode) along the slot and is given by

$$P_f = \int_x\int_{y \text{ plane}} (E_x H_y^* - E_y H_x^*)\, dx\, dy = \frac{1}{2\pi}\int_\alpha\int_{y \text{ plane}} (\tilde{E}_x \tilde{H}_y^* - \tilde{E}_y \tilde{H}_x^*)\, d\alpha\, dy \tag{3}$$

where E_x, E_y, H_x, H_y are fields tangential to the z-constant plane, and $*$ denotes the complex conjugate. The second equality in (3) follows from Parseval's theorem.

Manuscript received August 20, 1985; revised February 24, 1986. This work was supported in part by NASA Langley Research Center under Grant NAG-1-279.

The authors are with the Department of Electrical and Computer Engineering, University of Massachusetts, Amherst, MA 01003.

IEEE Log Number 8608831.

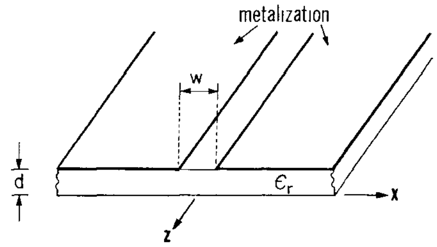

Fig. 1. Geometry of slotline.

TABLE I
Comparison of Calculated Slot Characteristic Impedance Z_0

ϵ_r	d/λ_0	W/d	$Z_0(\Omega)$ From curves in [3]	$Z_0(\Omega)$ Present
9.6	0.06	1.0	140	142
11.0	0.04	1.5	160	160
13 0	0.03	0 4	80	82
16 0	0.025	2 0	150	151
20.0	0.03	1.0	100	101

The fields $\tilde{E}$ and $\tilde{H}$ in the spectral domain pertaining to the air and dielectric regions of the slotline can be related to the aperture field (i.e., field in the slot), which is modeled by the method of moments. As was done in [1], the field in the slot region is expanded as

$$E_x^s = \sum_{n=0}^{M_x} a_n e_n^x$$

$$e_n^x = \left(\frac{2}{\pi W}\right)\frac{T_{2n}\left(\frac{2x}{W}\right)}{\sqrt{1-\left(\frac{2x}{W}\right)^2}}, \qquad n = 0,1,\cdots \tag{4}$$

$$E_z^s = \sum_{m=1}^{M_z} b_m e_m^z$$

$$e_m^z = \left(\frac{2}{\pi W}\right)\sqrt{1-\left(\frac{2x}{W}\right)^2}\, U_{2m-1}\left(\frac{2x}{W}\right), \qquad m = 1,2,\cdots \tag{5}$$

where T_n and U_n are Chebyshev polynomials of the first and second kind, respectively.

The Fourier transforms of the above basis functions can be found readily in closed form as [8]

$$\tilde{e}_n^x = (-1)^n J_{2n}\left(\frac{\alpha W}{2}\right), \qquad n = 0,1,\cdots \tag{6}$$

$$\tilde{e}_m^z = j(-1)^{m+1} 2m \frac{J_{2m}\left(\frac{\alpha W}{2}\right)}{\left(\frac{\alpha W}{2}\right)}, \qquad m = 1,2,\cdots. \tag{7}$$

The integration with respect to y in (3) can be done in closed form. However, the integration on the α variable must be done numerically. The slot wavelength λ' is stationary with respect to the slot field, and it was found that λ' converges with only one basis function for the longitudinal field as reported in [1]. However, more than one basis function for E_z^s is needed for the convergence of the characteristic impedance Z_0 for a wide slot. The maximum number of basis functions needed for E_x^s and E_z^s

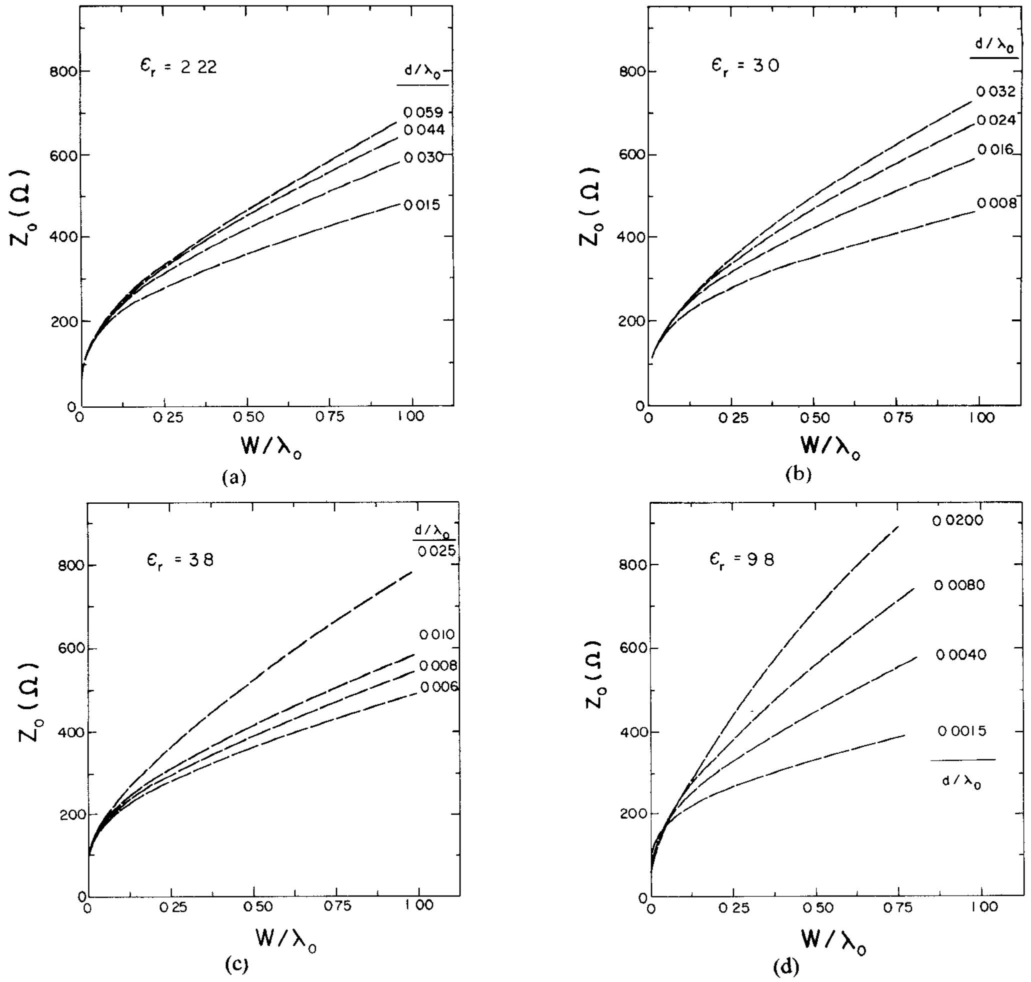

Fig. 2. Characteristic impedance of slotline as a function of normalized slot width. (a) $\epsilon_r = 2.22$. (b) $\epsilon_r = 3.0$. (c) $\epsilon_r = 3.8$. (d) $\epsilon_r = 9.8$.

during the computation of Z_0 was 5 and 3, respectively, when the slot width approached one free space wavelength λ_0.

Computer programs have been developed to compute λ' and Z_0 for a specified ϵ_r, λ_0, and d. As a check of these programs, Table I shows a comparison for Z_0 between the present computations and those in [3]. Characteristic impedances for slotlines have been computed for $\epsilon_r = 2.22$, 3.0, 3.8, 6.5, and 9.8 and for widths varying over $0.0015 \leqslant W/\lambda_0 \leqslant 1.0$. Computed values of Z_0 versus W/λ_0 with d/λ_0 as a parameter are plotted in Fig. 2.

Empirical formulas have been developed for the normalized slot wavelength λ'/λ_0 and the slot characteristic impedance Z_0 and are given in (8)–(15). These formulas have been obtained by least-square curve fitting the computed data. In each case, the average of the absolute percentage error "av" and the maximum percentage error "max," observed in a systematic sample of 120 data points, are given. Also, where possible, the region around which the maximum error has been observed is indicated.

The following formulas are all valid within $0.006 \leqslant d/\lambda_0 \leqslant 0.060$.

$$2.22 \leqslant \epsilon_r \leqslant 3.8$$

$$0.0015 \leqslant W/\lambda_0 \leqslant 0.075$$

$$\lambda'/\lambda_0 = 1.045 - 0.365 \ln \epsilon_r + \frac{6.3 (W/d)\epsilon_r^{0.945}}{(238.64 + 100 W/d)} - \left[0.148 - \frac{8.81(\epsilon_r + 0.95)}{100\epsilon_r}\right] \cdot \ln(d/\lambda_0). \quad (8)$$

av = 0.37 percent, max = 2.2 percent (at one point)

$$Z_0 = 60. + 3.69 \sin\left[\frac{(\epsilon_r - 2.22)\pi}{2.36}\right] + 133.5 \ln(10\epsilon_r)\sqrt{W/\lambda_0} + 2.81[1 - 0.011\epsilon_r(4.48 + \ln \epsilon_r)](W/d)\ln(100 d/\lambda_0) + 131.1(1.028 - \ln \epsilon_r)\sqrt{d/\lambda_0} + 12.48(1 + 0.18 \ln \epsilon_r)\frac{W/d}{\sqrt{\epsilon_r - 2.06 + 0.85(W/d)^2}}. \quad (9)$$

av = 0.67 percent, max = 2.7 percent (at one point)

$$0.075 \leqslant W/\lambda_0 \leqslant 1.0$$

$$\lambda'/\lambda_0 = 1.194 - 0.24 \ln \epsilon_r - \frac{0.621\epsilon_r^{0.835}(W/\lambda_0)^{0.48}}{(1.344 + W/d)} - 0.0617\left[1.91 - \frac{(\epsilon_r + 2)}{\epsilon_r}\right]\ln(d/\lambda_0) \quad (10)$$

av = 0.69 percent, max = −2.6 percent (at two points, for $W/\lambda_0 > 0.8$)

$$Z_0 = 133 + 10.34(\epsilon_r - 1.8)^2 + 2.87\left[2.96 + (\epsilon_r - 1.582)^2\right] \cdot \left[\{W/d + 2.32\epsilon_r - 0.56\} \cdot \{(32.5 - 6.67\epsilon_r)(100 d/\lambda_0)^2 - 1\}\right]^{1/2} - (684.45 d/\lambda_0)(\epsilon_r + 1.35)^2 + 13.23[(\epsilon_r - 1.722) W/\lambda_0]^2 \quad (11)$$

av = 1.9 percent, |max| = 5.4 percent (at three points, for $W/\lambda_0 > 0.8$)

$$3.8 \leqslant \epsilon_r \leqslant 9.8$$
$$0.0015 \leqslant W/\lambda_0 \leqslant 0.075$$

$$\lambda'/\lambda_0 = 0.9217 - 0.277\ln\epsilon_r + 0.0322(W/d)\left[\frac{\epsilon_r}{(W/d + 0.435)}\right]^{1/2} - 0.01\ln(d/\lambda_0)\left[4.6 - \frac{3.65}{\epsilon_r^2\sqrt{W/\lambda_0}(9.06 - 100W/\lambda_0)}\right] \quad (12)$$

av = 0.6 percent, |max| = 3 percent (at three points, occurs for $W/d > 1$ and $\epsilon_r > 6.0$)

$$Z_0 = 73.6 - 2.15\epsilon_r + (638.9 - 31.37\epsilon_r)(W/\lambda_0)^{0.6} + \left(36.23\sqrt{\epsilon_r^2 + 41} - 225\right)\frac{W/d}{(W/d + 0.876\epsilon_r - 2)} + 0.51(\epsilon_r + 2.12)(W/d)\ln(100d/\lambda_0) - 0.753\epsilon_r(d/\lambda_0)/\sqrt{W/\lambda_0} \quad (13)$$

av = 1.58 percent, max = 5.4 percent (at three points, occurs for $W/d > 1.67$)

$$0.075 \leqslant W/\lambda_0 \leqslant 1.0$$

$$\lambda'/\lambda_0 = 1.05 - 0.04\epsilon_r + 1.411\times10^{-2}(\epsilon_r - 1.421)\cdot\ln\{W/d - 2.012(1 - 0.146\epsilon_r)\} + 0.111(1 - 0.366\epsilon_r)\sqrt{W/\lambda_0} + 0.139(1 + 0.52\epsilon_r\ln(14.7 - \epsilon_r))(d/\lambda_0)\ln(d/\lambda_0) \quad (14)$$

av = 0.75 percent, |max| = 3.2 percent (at two points, occurs for $W/\lambda_0 = 0.075$, $d/\lambda_0 > 0.03$)

$$Z_0 = 120.75 - 3.74\epsilon_r + 50\left[\tan^{-1}(2\epsilon_r) - 0.8\right]\cdot(W/d)^{[1.11 + (0.132(\epsilon_r - 27.7)/(100d/\lambda_0 + 5))]}\cdot\ln\left[100d/\lambda_0 + \sqrt{(100d/\lambda_0)^2 + 1}\right] + 14.21(1 - 0.458\epsilon_r)(100d/\lambda_0 + 5.1\ln\epsilon_r - 13.1)\cdot(W/\lambda_0 + 0.33)^2 \quad (15)$$

av = 2.0 percent, |max| = 5.8 percent (at two points, occurs for $W/\lambda_0 < 0.1$). In the above formula, $\tan^{-1}(\cdot)$ assumes its principal value.

III. Conclusion

A spectral-domain Galerkin method is used to compute the characteristic impedance of wide slotlines on low-ϵ_r substrates. Empirical formulas have been presented for the slot wavelength and the characteristic impedance over a wide range of slot widths. The data presented here supplement data already available on high-ϵ_r substrates.

References

[1] R. Janaswamy and D. H. Schaubert, "Dispersion characteristics for wide slotlines on low permittivity substrates," *IEEE Trans. Microwave Theory Tech.*, vol. MTT-33, pp. 723–726, Aug. 1985.

[2] J. B. Knorr and K. Kuchler, "Analysis of coupled slots and coplanar strips on dielectric substrate," *IEEE Trans. Microwave Theory Tech.*, vol. MTT-23, pp. 541–548, July 1975.

[3] E. A. Mariani *et al.*, "Slotline characteristics," *IEEE Trans. Microwave Theory Tech.*, vol. MTT-17, pp. 1091–1096, Dec. 1969.

[4] E. L. Kollberg *et al.*, "New results on tapered slot endfire antennas on dielectric substrate," presented at the 8th IEEE Int. Conf. Infrared, Millimeter Waves, Miami, FL, Dec. 1983.

[5] S. N. Prasad and S. Mahapatra, "A new MIC slot line, aerial," *IEEE Trans. Antennas Propagat.*, vol. AP-31, pp. 525–527, May 1983.

[6] J. F. Johansson, "Investigation of some slotline antennas," M.S. thesis, Chalmers University, Gothenberg, Sweden, 1983.

[7] T. Itoh and R. Mittra, "Dispersion characteristics of slot lines," *Electron. Lett.*, vol. 7, pp. 364–365, July 1971.

[8] A. Erdelyi *et al.*, *Tables of Integral Transforms*, vol. 2. New York: McGraw-Hill, 1954.

A Broad-Band Homodyne Network Analyzer with Binary Phase Modulation

UWE GÄRTNER, MEMBER, IEEE, AND BURKHARD SCHIEK, MEMBER, IEEE

***Abstract*—An automatic homodyne network analyzer system using cascaded binary phase shifters is described which operates over the full *X*-band with a high dynamic range due to an auxiliary modulation and linear detection technique. A general analytic solution of the complex nonlinear system equations is given which allows the use of a coupled modulator/phase shifter structure. Measurement results are reported.**

Nomenclature

B_u, B_l	Modulator conversion losses for the first upper and lower sidebands.
$\tilde{B}_u, \tilde{B}_l$	Modified modulator conversion losses in case of a coupling to phase shifter 1.
H	Transfer function of the device under test; $H = \alpha_{DUT}\, e^{j\Psi DUT}$.
H_R	Weighted linear combination of all or a subset of the complex IF amplitudes V_n, $n = 1,\cdots,8$, for an evaluation of H; ideally, $H_R = \tilde{K}H$; $\tilde{K} \triangleq$ system constant.
$K, K_0, \tilde{K}$	System constants.
$k_i, i = 1,2,3$	Characteristic of binary phase shifter PSi, i.e., $\lvert k_i\rvert \triangleq$ insertion loss change, $\arg\{k_i\} = \Delta\Phi \triangleq$ differential phase shift.
k_{iu}, k_{il}	Characteristic of PSi for the first upper and lower sideband frequencies.
$\tilde{k}_{1u}, \tilde{k}_{1l}$	Modified characteristic of PS1 in case of a coupling to modulator M.
P_{RF}	Double-sideband mixer input power level.
$p_i, i = 1,2,3$	Weighting factors for the determination of the transfer function H through H_R.
$V_n, n = 1,\cdots,8$	Complex amplitude of the IF output signal for the eight switching-state combinations of PS1, PS2, and PS3.

Auxiliary Variables

$$\tilde{B} = B_u + B_l$$
$$\tilde{k}_1 = B_u/\tilde{B}\cdot k_{1u} + B_l/\tilde{B}\cdot k_{1l}$$
$$\tilde{\tilde{B}} = B_u - B_l$$
$$\tilde{\tilde{k}}_1 = B_u/\tilde{\tilde{B}}\cdot k_{1u} - B_l/\tilde{\tilde{B}}\cdot k_{1l}$$
$$U_n = 2\,\mathrm{Re}\{V_n\}, n = 1,\cdots,8$$
$$I_n = 2j\,\mathrm{Im}\{V_n\}, n = 1,\cdots,8$$

Manuscript received January 27, 1986; revised March 5, 1986. This work was supported in part by the Deutsche Forschungsgemeinschaft.

The authors are with the Institut für Hoch- und Höchstfrequenztechnik, Ruhr-Universität Bochum, D-4630 Bochum, Federal Republic of Germany.

IEEE Log Number 8609060.